JCI The Journal of Clinical Investigation

Amendment history:
- Corrigendum (June 2022)

Mass cytometry detects H3.3K27M-specific vaccine responses in diffuse midline glioma

Sabine Mueller, Jared M. Taitt, Javier E. Villanueva-Meyer, Erin R. Bonner, Takahide Nejo, Rishi R Lulla, Stewart Goldman, Anu Banerjee, Susan N. Chi, Nicholas S. Whipple, John R. Crawford, Karen Gauvain, Kellie J. Nazemi, Payal B. Watchmaker, Neil D. Almeida, Kaori Okada, Andres M. Salazar, Ryan D. Gilbert, Javad Nazarian, Annette M. Molinaro, Lisa H. Butterfield, Michael D. Prados, Hideho Okada

J Clin Invest. 2020. https://doi.org/10.1172/JCI140378.

Clinical Research and Public Health In-Press Preview **Immunology** **Oncology**

Background:

Patients with diffuse midline gliomas (DMG), including diffuse intrinsic pontine glioma (DIPG), have dismal outcomes. We previously described the H3.3K27M mutation as a shared neoantigen in HLA-A*02.01$^+$ H3.3K27M$^+$ DMGs. Within the Pacific Pediatric Neuro-Oncology Consortium, we assessed safety and efficacy of an H3.3K27M-targeted peptide vaccine.

Patients and Methods:

Newly diagnosed patients aged 3-21 years with HLA-A*02.01$^+$ and H3.3K27M$^+$ status were enrolled into Stratum A (DIPG) and Stratum B (non-pontine DMG). Vaccine was administered in combination with poly-ICLC every three weeks for eight cycles, followed by once every six weeks. Immuno-monitoring and imaging occurred every three months. Imaging was centrally reviewed. Immunological responses were assessed in peripheral blood mononuclear cells using mass cytometry.

Results:

19 patients enrolled in Stratum A (median age=11 years) and 10 in Stratum B (median age=13 years). There were no grade 4 treatment-related adverse events (TRAE). Injection site reaction was the most commonly reported TRAE. Overall survival (OS) at 12 months was 40% (95% CI, 22% to 73%) for Stratum A and 39% (95% CI, 16% to 93%) for Stratum B. The median OS was 16.1 months in patients exhibiting an expansion of H3.3K27M-reactive CD8$^+$ T-cells […]

TITLE PAGE

Mass cytometry detects H3.3K27M-specific vaccine responses in diffuse midline glioma

Sabine Mueller*[1, 2, 3, 4], Jared M. Taitt*[,2], Javier E. Villanueva-Meyer[5], Erin R. Bonner[6], Takahide Nejo[2], Rishi R. Lulla[7], Stewart Goldman[8], Anu Banerjee [2,3], Susan N. Chi[9], Nicholas S. Whipple[10], John R. Crawford[11], Karen Gauvain[12], Kellie J. Nazemi[13], Payal B. Watchmaker[2], Neil D. Almeida[14], Kaori Okada[2], Andres M. Salazar[15], Ryan D. Gilbert[2], Javad Nazarian[4,6], Annette M. Molinaro[2], Lisa H. Butterfield[16,17], Michael D. Prados[2,3] and Hideho Okada[2,16]

[1]Department of Neurology, [2]Neurosurgery and [3]Pediatrics, University of California, San Francisco

[4]Children's University Hospital Zurich, Switzerland

[5]Department of Radiology and Biomedical Imaging, University of California, San Francisco

[6]Children's National Medical Center, Washington DC

[7]Division of Pediatric Hematology/Oncology, Hasbro Children's Hospital, Department of Pediatrics, The Warren Alpert Medical School of Brown University, Providence, RI

[8]Ann & Robert H. Lurie Children's Hospital of Chicago

[9]Dana-Farber Cancer Institute, Boston, MA

[10]Division of Hematology/Oncology, Department of Pediatrics, University of Utah, Salt Lake City, UT

[11]Department of Neurosciences and Pediatrics, University of California, San Diego and Rady Children's Hospital, San Diego

[12]St. Louis Children's Hospital, Washington University in St. Louis

[13]Doernbecher Children's Hospital, Oregon Health & Science University

[14]The George Washington University School of Medicine and Health Sciences, The George Washington University, Washington, District of Columbia, USA

[15]Oncovir Inc., Washington DC

[16]Parker Institute for Cancer Immunotherapy, San Francisco

[17]Department of Microbiology and Immunology, University of California, San Francisco

*These authors contributed equally to this manuscript

SM, MP and HO conceptualized and designed the study. JT, TN, PW, NA, KO LB and RG analyzed PBMC and tumor tissue samples. JVM conducted imaging data analyses. EB and JN evaluated ctDNA. SM, RL, SG, AB, SC, NW, JC, KG and KN enrolled and managed patients. AS provided poly-ICLC. AM supervised statistical and analytical methods. All authors participated in writing and revisions of the manuscript.

This work has been partially presented at the 5th Biennial Conference on Pediatric Neuro-Oncology Basic and Translational Research (2019) as well as the 24th Annual Meeting and Education Day of the Society for Neuro-Oncology (2019).

Corresponding author:

Hideho Okada, MD, PhD

Neurological Surgery

University of California San Francisco

Helen Diller Family Cancer Research Building HD 472

1450 3rd Street San Francisco, CA 94158

Email: hideho.okada@ucsf.edu

Phone: (415)476-1637

Conflict of Interests Statement

Hideho Okada is an inventor of a Utility Patent Application Titled “H3.3 CTL peptides and uses thereof” (Attorney Docket No: 81906-938904-220400 US, Client Reference No. SF15-163) which has been exclusively licensed to Tmunity Therapeutics, Inc.

Funding: V Foundation, the Pacific Pediatric Neuro-Oncology Consortium Foundation, The Pediatric Brain Tumor Foundation, Mithil Prasad Foundation, The MCJ Amelior Foundation, Anne and Jason Farber Foundation, Will Power Research Fund Inc., Isabella Kerr Molina Foundation, Parker Institute for Cancer Immunotherapy, NIH/NINDS R35 NS105068 (HO)

Abstract

Background:

Patients with diffuse midline gliomas (DMG), including diffuse intrinsic pontine glioma (DIPG), have dismal outcomes. We previously described the H3.3K27M mutation as a shared neoantigen in HLA-A*02.01^{+} H3.3K27M^{+} DMGs. Within the Pacific Pediatric Neuro-Oncology Consortium, we assessed safety and efficacy of an H3.3K27M-targeted peptide vaccine.

Patients and Methods:

Newly diagnosed patients aged 3-21 years with HLA-A*02.01^{+} and H3.3K27M^{+} status were enrolled into Stratum A (DIPG) and Stratum B (non-pontine DMG). Vaccine was administered in combination with poly-ICLC every three weeks for eight cycles, followed by once every six weeks. Immuno-monitoring and imaging occurred every three months. Imaging was centrally reviewed. Immunological responses were assessed in peripheral blood mononuclear cells using mass cytometry.

Results:

19 patients enrolled in Stratum A (median age=11 years) and 10 in Stratum B (median age=13 years). There were no grade 4 treatment-related adverse events (TRAE). Injection site reaction was the most commonly reported TRAE. Overall survival (OS) at 12 months was 40% (95% CI, 22% to 73%) for Stratum A and 39% (95% CI, 16% to 93%) for Stratum B. The median OS was 16.1 months in patients exhibiting an expansion of H3.3K27M-reactive CD8^{+} T-cells compared to 9.8 months for their counterparts (p=0.05). DIPG patients with below-median baseline levels of myeloid-

derived suppressor cells had prolonged OS compared to their counterparts ($p<0.01$). Immediate pre-treatment dexamethasone administration inversely associated with H3.3K27M-reactive $CD8^+$ T-cell responses.

Conclusion:

Administration of the H3.3K27M-specific vaccine is well tolerated. Patients with H3.3K27M-specific $CD8^+$ immunological responses demonstrated prolonged OS compared to non-responders.

Trial Registration: ClinicalTrials.gov NCT 02960230

Introduction

Diffuse midline gliomas (DMGs) are uniformly fatal pediatric brain cancers, and despite maximal therapy, survival outcomes remain dismal with less than 10% of patients surviving beyond two years (1). A hallmark of DMGs is a set of recurrent mutations in genes encoding histone H3 variants including histone H3.3 (*H3F3A*) and H3.1 (*HIST1H3B* and *HIST1H3C*) (2, 3). Recently, immunotherapy has gained significant attention as a treatment for cancers harboring tumor-specific neoantigens. We have identified a 10-mer peptide spanning position 26-35 (H3.3K27M$_{26\text{-}35}$) of the H3.3K27M protein as a human leukocyte antigen (HLA)-A*02:01-restricted cytotoxic T lymphocyte (CTL) epitope (4). While most missense mutation-derived neoantigens are unique to individual patients (5), a majority of DMG and more than 70% of diffuse intrinsic pontine glioma (DIPG) cases exhibit the H3.3K27M mutation (6). The H3.3K27M-derived neoantigen epitope represents a valuable target as it is not only tumor-specific, but also K27M mutant protein is present throughout all tumor nuclei in each of the 47 cases evaluated by immunohistochemistry (7), suggesting that this may be a truncal mutation and less likely to lead to antigen-loss mediated escape of the tumor. Within this multicenter study conducted through the Pacific Pediatric Neuro-Oncology Consortium (PNOC), we evaluated the safety, immunoreactivity, and efficacy of synthetic H3.3K27M$_{26\text{-}35}$ peptide in combination with helper tetanus toxoid (TT) peptide and poly-ICLC adjuvant in patients with HLA-A*02:01^{+}, H3.3K27M^{+} DMGs.

Results

Patient Characteristics

From November 2016 until March 2019, 19 eligible patients (median age=11, IQR=4.5 years; 53% female) were enrolled in Stratum A and 10 eligible patients (median age=13, IQR=4.25 years; 60% female) in Stratum B (**Table 1**). DMGs in Stratum B included seven thalamic tumors, two pontine-centered tumors that did not meet imaging criteria for DIPG, with extension into the cerebellum in both and the cervical spine in one, and one spinal cord tumor located within the thoracic spine. Median time between tumor tissue collection and start of RT was 17 days (range=4-25 days) for Stratum A and 22 days (range=2-49 days) for Stratum B, except for one patient who had a biopsy performed after RT completion. Median time from completion of RT to first vaccine was 39 days (range=27-71 days) for Stratum A and 39 days (range=22-53 days) for Stratum B.

Treatment and Safety

The median number of vaccinations administered was seven (IQR=4) and five (IQR=4.5) for Strata A and B, respectively. Treatment was generally well tolerated with no grade 4 treatment-related adverse events (TRAEs). The most common TRAE included injection site reaction (**Table 2**). One patient from Stratum A experienced a regimen-limiting toxicity (RLT), presenting with signs and symptoms of meningitis. This patient was treated per institutional guidelines with antibiotics and was hospitalized until recovery. Blood and cerebrospinal fluid remained negative, though the patient was started on antibiotics prior to collection. After recovery from this event, the patient was

taken off study as TRAEs could not be excluded. There were no other instances of meningitis.

Clinical Efficacy

The primary efficacy endpoint was the overall survival at 12 months (OS12) of patients in stratum A. With a median follow-up time of 17.6 months, the OS12 rate was 44% (95% CI, 27% to 75%) for Stratum A and 39% (95% CI, 16% to 93%) for Stratum B (**Figure 1A**). Median PFS was 4.9 months (95% CI, 3 to 8.3 months) for Stratum A and 3.5 months (95% CI, 3 to N/A) for Stratum B (**Figure 1B**). There was one case of positive response (partial response; PNOC007-25) in stratum A.

Detection, Validation, Clustering, and Phenotyping of H3.3K27M-reactive CD8$^+$ T-Cells

CyTOF-based immune analyses were conducted on 28 of the total 29 patients enrolled in the study, where H3.3K27M-reactive CD8$^+$ T-cells were detected using a conventional CD8$^+$ gating strategy (Data Supplement; Figure S1). H3.3K27M-dextramer staining exhibited negligible non-specific staining on healthy donor-derived PBMCs (**Figure 1C**). CyTOF-based H3.3K27M-reactive CD8$^+$ T-cell detection was determined to be as sensitive as flow cytometry (Data Supplement; Figure S2). H3.3K27M-reactive CD8$^+$ T-cells were clustered on a tSNE plot and grouped into five subpopulations (Data Supplement; Figure S3): early activated (T_{EA}), stem cell memory (T_{SCM}), effector (T_{EFF}), effector memory (T_{EM}), and exhausted (T_{EX}) phenotypes based on their aggregate phenotypic profiles (**Figure 1D**; Supplementary Methods).

Expansion of H3.3K27M-reactive CD8$^+$ T-Cells is Associated with Better Prognosis

Of the patients from whom multiple PBMC time points were collected (n=18), longitudinal H3.3K27M-reactive CD8+ T-cell frequencies were analyzed (Data Supplement; Figure S4), revealing seven (39%) patients meeting the criteria of an immunological response (**Figure 1E**). Among these patients, the median OS of overall immunological responders was 16.3 months (n=7, 95% CI, 12.6 to N/A), compared to 9.9 months (n=11, 95% CI, 9.0 to N/A) for non-responders (p=0.05, log-rank) (**Figure 1F**) with an estimated multivariate HR of 0.04 (95% CI, 0.004 to 0.045, p<0.01) (Data Supplement; Table S1). Further, immunological responders exhibited prolonged PFS (p=0.05, log-rank) compared to non-responders (**Figure 1G**). Patients with T_{EM} (n=6, p=0.02, log-rank) expansions also exhibited trends towards prolonged OS (**Figure 1H**; Data Supplement; Figure S5) and PFS (p=0.06, log-rank) compared to their counterparts (**Figure 1I**; Data Supplement; Figure S6). These trends persisted when controlling for stratum, as DIPG patients exhibiting overall immunological responses had a median OS of 16.1 months (n=6, 95% CI, 12.4 to N/A) compared to 10 months (n=6, 95% CI, 9.5 to N/A) for non-responders (p=0.11, log-rank) (Data Supplement; Figure S7) with an estimated multivariate HR of 0.03 (95% CI, 0.001 to 1.960, p=0.10) (Data Supplement; Table S1). Prolonged OS among DIPG patients with T_{EM} expansions (n=6, p=0.03, log-rank) further strengthened this association, while also being substantiated by prolonged PFS (p<0.01, log-rank) relative to non-responders (Data Supplement; Figure S8). These corroborating survival trends did not persist when using the same longitudinal immunological response threshold for bulk CD8+ T-cell phenotypic

subtypes (Data Supplement; Figure S9, S10, S11, and S12), suggesting that the survival benefit associated with the expansion of H3.3K27M-reactive CD8+ T-cells is independent of overall T-cell status. No association between H3.3K27M-reactive T_{EX} expansion and patient outcomes was established (Data Supplement; Figures S5, S6, S7, and S8). The number of vaccines administered correlated with the longitudinal percent change of H3.3K27M-reactive $CD8^+$ T-cells at the final time point analyzed relative to baseline (Data Supplement; Figure S13). However, the median number of vaccines preceding immunological responses was 6 (IQR=2) among responders whereas the median number of total vaccines was also 6 (IQR=4) among non-responders (**Figure 2**), suggesting that the number of vaccines is not a sole factor for separating responders vs. non-responders.

Circulatory MDSC Abundance at Baseline Functions as a Prognostic Indicator for DIPG Patients

Myeloid cells were identified using a conventional myeloid gating strategy (**Figure 3A**). Of these clusters, E-MDSC ($CD33^+$ $CD11b^+$ HLA-DR^{lo} Lin^{lo}) and M-MDSC ($CD33^+$ $CD11b^+$ $CD14^+$ HLA-DR^{lo}) could be distinguished using their phenotypic profiles (Data Supplement; Figure S14, Table S2). Patients were stratified into $MDSC^{lo}$ and $MDSC^{hi}$ cohorts (**Figure 3B**) for each subpopulation. While baseline E-MDSC abundance did not correlate with improved outcomes (Data Supplement; Figures S15 and S16), M-$MDSC^{lo}$ patients displayed prolonged OS (p=0.05, log-rank) relative to the M-$MDSC^{hi}$ cohort among DIPG patients (Data Supplement; Figure S16). $MDSC^{lo}$ patients had median OS of 13.7 months (95% CI, 9.8 to N/A), compared to 9.0 months (95% CI, 7.7 to N/A) in $MDSC^{hi}$ DIPG patients (p<0.01, log-rank) (**Figure 3C**) with an estimated

multivariate HR of 0.09 (95% CI, 0.01 to 0.92, p=0.04) (Data Supplement; Table S1). Further, $MDSC^{hi}$ patients had a median PFS of 2.9 months (95% CI, 2.8 to N/A), compared to 5.3 months (95% CI, 3.2 to N/A) for their counterparts (p=0.03, log-rank) (**Figure 3D**) with an estimated univariate HR of 3.1 (95% CI, 1.1 to 8.9, p=0.04). Analyses incorporating both Strata A and B did not yield significant findings (Data Supplement; Figure S15), while the limited sample size of stratum B prevented a robust cohort-specific survival analysis for these patients. These associations persisted when analyzing the outcomes of patients exhibiting the top and bottom quartile of baseline MDSC abundances (Data Supplement; Figure S17). However, baseline MDSC frequencies did not correlate with tumor volume or age (Data Supplement; Figure S18). In regard to other immunoregulatory populations, $CD4^+$ regulatory T-cells (Tregs) posed negligible associations with patient outcomes in the DIPG cohort (Data Supplement; Figure S19).

Dexamethasone Administration is Associated with Lower Rates of Vaccine-Specific $CD8^+$ T-Cell Responses and High MDSC Levels among DIPG Patients

A total of nine (47%) DIPG patients received oral dexamethasone while on study. Six of these patients commenced dexamethasone at least 3 days prior to baseline PBMC collection, and exhibited a trend towards higher levels of baseline circulatory MDSCs, while consisting of four (57%) of the seven patients with the highest circulatory MDSC levels of all analyzed patients (n=19) (**Figure 4A**). Among patients receiving dexamethasone who were analyzed longitudinally, three (50% of 6 total) exhibited an overall decrease in H3.3K27M-reactive $CD8^+$ T-cells at the final collection time point relative to baseline whereas only one (17% of 6 total) showed an overall expansion

(**Figure 4B**; Data Supplement; Figure S20). Furthermore, DIPG patients treated with dexamethasone at baseline had median OS of 9.0 months (n=6, 95% CI, 7.7 to N/A) compared to median OS of 13.7 months (n=13, 95% CI, 9.8 to N/A) among untreated patients (p<0.01, log-rank) (**Figure 4C**). While not statistically significant, DIPG patients treated with dexamethasone had median PFS of 3.0 months (n=6, 95% CI, 2.3 to N/A) compared to median PFS of 5.3 (n=13, 95% CI, 4.1 to N/A) among untreated patients (p=0.09, log-rank) (**Figure 4D**). These trends persisted when combining Strata A and B (Data Supplement; Figure S21).

Circulating Tumor DNA Analysis is Not Predictive of Outcome

A cutoff threshold for positive circulating tumor DNA (ctDNA) was set at 0.001% based on our previously described method (8), where sensitivity and specificity were fully described using a large cohort of patient specimens. At baseline, 27/29 patients had plasma collected to quantify H3.3K27M mutation (*H3F3A* c.83A>T) allelic frequency (MAF) (8-10). Circulating *H3F3A* c.83A>T tumor DNA H3.3K27M-specific ctDNA was detected in 70.4% (n=19/27) of patient samples, but its presence at baseline or longitudinal fluctuation in abundance did not correlate with clinical outcomes (Data supplement; Figures S22 and S23) or immunological responses (Taitt, unpublished observations).

Longitudinal Assessment of Immunological Profiles in Correlation to Clinical Outcome of a DIPG Patient Exhibiting Strong CD8$^+$ Response to Vaccination

One patient enrolled in Stratum A demonstrated partial radiographic response at weeks

12 and 24 (**Figure 5A**). Following a total of nine vaccinations, the patient was taken off study at week 36 due to clinical worsening but only minor increase in tumor size, which did not meet radiographic progression criteria based on central imaging review. The patient received re-irradiation 10 months after the first vaccine and never received dexamethasone. The patient has not received additional therapies and remains alive 19 months after initial diagnosis (March 2020 cutoff). Longitudinal immunological assessment revealed the time course-dependent expansion and persistence of H3.3K27M-reactive $CD8^+$ T-cells (**Figure 5B**). The continuously mounting T-cell responses along with the minor increase of tumor size at week 36 suggest a possibility of inflammation-associated imaging change in this case. This patient was classified as $MDSC^{lo}$ among DIPG patients with total MDSC levels of 2.6% (median=4.2%), indicative of improved prognosis among DIPG patients as our findings have reflected (**Figure 3C**, **Figure 3D**). Further, this patient's MDSC abundance did not increase above median levels until disease progression was identified at 36 weeks (**Figure 5C**).

Discussion

This is the first multi-center trial assessing the safety and clinical efficacy of a vaccine directed towards the novel, shared neoantigen H3.3K27M $_{(27\text{-}26)}$ in HLA-A*02:01$^+$ patients with H3.3K27M$^+$ DIPG/DMG. The study demonstrated safety of the regimen and supports the significance of immunological monitoring for identification of predictive biomarkers. Moreover, clinical and immune data suggest concurrent corticosteroid administration is associated with increased MDSC levels and lower vaccine efficacy.

The PNOC007 trial regimen demonstrated safety in regard to expected TRAEs. One child developed meningitis of unclear etiology that recovered completely with standard treatment. It remains uncertain if this event was related to the vaccine since no further cases were identified. The PNOC007 treatment strategy did not improve the overall outcome of H3.3K27M^{+} DMG patients, representing the worst prognostic group among DMGs (11). A recent analysis from the International and European DIPG registries reported a similar OS12 of 42.3% (95% CI, 38.1% to 44.1%) (1).

To our knowledge this is the first trial whereby individuals with DMGs were enrolled based on mutation status rather than location. Outcome measures for these tumors remain a topic of ongoing prospective studies, but retrospective reviews show poor outcomes for these location-specific subgroups. For example, a retrospective analysis of H3.3K27M^{+} DMGs enrolled in the German HIT-HGG registry demonstrated a median survival of 13 months among thalamic tumors and 4.8 months among tumors within the spine (11), similar to our results. To date, very few peptide vaccine-based strategies have been reported for DIPGs/DMGs. We have previously reported a median survival of 12.7 months in DIPG patients using a peptide vaccine strategy against IL-13Rα, EphA2, and survivin in combination with poly-ICLC (12). This trial employed a similar strategy to PNOC007; however, H3.3K27M status was not available and could have influenced outcomes.

Our CyTOF-based analyses of multiple immune subsets (13, 14) provided an opportunity to explore associations between expansion of H3.3K27M-reactive CD8^{+} T-cell subsets and prolonged OS and PFS. Furthermore, this approach identified baseline circulatory MDSCs as a potential negative prognostic indicator for DIPG patients. To our

knowledge, this is the first CyTOF-based immuno-monitoring platform utilized to evaluate epitope-specific $CD8^+$ T-cell responses in cancer patients treated with peptide-based vaccines. Detection of this cell population was accomplished through HLA-dextramer-based staining (15-17), as dextramers exhibit higher affinity and specificity for epitope-specific $CD8^+$ T-cell populations in comparison to conventional HLA-tetramers (15, 17). Furthermore, an increased quantity of fluorophores conjugated to each dextramer allowed for increased binding to metal-conjugated secondary antibodies, resulting in higher resolution on both fluorophore and lanthanide-based analytical platforms. This approach maximized sensitivity on the CyTOF platform, allowing for the comparable detection of H3.3K27M-reactive $CD8^+$ T-cells between flow and mass cytometry. This study validates CyTOF as a powerful tool for high-definition immuno-monitoring of $CD8^+$ T-cell-based immunotherapies.

While other immune populations receive interest (18, 19) across the broad spectrum of cancer vaccines (20), $CD8^+$ T-cells remain the primary target population for eliciting an efficacious antitumor immunotherapy (21). Consistent with this paradigm, the expansion of H3.3K27M-reactive $CD8^+$ T-cells, but not bulk CD8+ T-cells, is suggestive of prolonged OS. While this expansion provides insight into patient-specific immunological outcomes, it does not account for phenotypic composition and functionality. As peripheral T_{EX} expansion has been correlated with poor prognoses in several cancer types (22, 23), the discrimination of this population, among others, is necessary for a contextual assessment of immunological responses. Our data demonstrated no association between T_{EX} expansion and favorable outcomes for patients. However, the expansion of H3.3K27M-reactive T_{EM} subpopulations, which exhibit cytolytic and tissue

localization capabilities (24), was associated with clinical benefits among DMG patients, consistent with previous reports (25-27).

One could raise a concern whether the observed H3.3K27M-reactive $CD8^+$ T-cell responses merely reflect patient's overall immune competency which is often compromised in these patients. Our multivariate analysis on bulk $CD8^+$ T-cells suggested that this was not the case. Another line of concern is a possibility that patients with intrinsically slow-growing tumors may have received more vaccines than those with fast-growing tumors, thereby mounting higher levels of vaccine-reactive responses. Based on our analyses, this does not appear to be the case as the median numbers of vaccines preceding immunological responses among responders was the same as the median number of total vaccines among non-responders.

To date, there are no vaccine regimens that have been shown to be efficacious in CNS malignancies based on randomized studies with adequate statistical powers. As we discussed in our recent review articles (28, 29), we recognize a number of mechanistic challenges underlying these failures, such as antigen-heterogeneity, local and systemic immunosuppression and lack of adequate homing of effector immune cells. While most tumor-specific antigens are expressed heterogeneously within the tumor (29), H3.3K27M appears to be uniformly expressed in the tumor tissue (7).

In terms of relevant immunosuppressive mechanisms, MDSCs attract particular interest as not only tumor-promoting (30) but as entities antagonistic to peptide vaccine efficacy (31-33) in preclinical models. Our data reflected this, as $MDSC^{lo}$ DIPG patients exhibited improved outcomes relative to their counterparts. It is also noteworthy that our data set showed an absence of associations between relative circulatory MDSC

abundance and both the patients' age and tumor volume. While Tregs are important immunosuppressive cells, our analyses did not detect any association between Tregs and patient outcomes in the DIPG cohort, corroborating recent high-throughput analyses of PBMC samples in glioblastoma patients (30). However, these results warrant caution. As cryopreservation and paraformaldehyde fixation are known to reduce polymorphonuclear MDSC viability (34), E-MDSC and M-MDSCs were used as a proxy for total MDSC quantification. Our data did not establish a robust correlation between baseline MDSC levels and longitudinal H3.3K27M-reactive CD8+ T-cell frequencies, which may have been impacted by the limited longitudinal samples available. Nevertheless, MDSCs represent an enticing target for combinatorial therapies (35) for maximizing vaccine efficacy.

Corticosteroids are often administered to DIPG/DMG patients to treat neurological dysfunction caused by tumor or treatment-related edema. However, steroid dependency has been associated with worse prognosis (36) and may negatively impact responses to immunotherapies (5). Consistent with recent preclinical in vitro and in vivo studies (37, 38), our data suggest a negative association between dexamethasone administration and the longitudinal expansion of vaccine-reactive $CD8^+$ T-cells, consistent with a recent report (5). It is conceivable that tumor size and growth rate, which typically necessitate use of corticosteroid, may confound our observations. Our data suggest a lack of association between the baseline tumor size and outcomes (Data Supplement; Figures S24 and S25), consistent with a recent study with molecularly-characterized DIPGs (39). However, given the small sample size, we cannot fully exclude that

dexamethasone use, independent of its impact on vaccine efficacy, leads to worse outcomes. Nonetheless, this association calls for additional corroborative studies.

Key limitations of our study include the relatively small number of patients and longitudinal samples for immune-phenotypic analyses and classification of immunological responses. Some study participants were lost to follow-up due to clinical worsening prior to post-baseline PBMC collection, limiting the availability of longitudinal samples to 62% (18/29) of the patients enrolled. Systematic evaluation of pre- and post-treatment tumor microenvironment samples would have offered more insights on vaccine effects, such as T-cell infiltration as well as possible antigen-loss and HLA-downregulation. To date, post-treatment biopsy of patients with DMGs remains a controversial topic in pediatric neuro-oncology (10, 40), and this limitation extended to our current study. At the time of submission, there were too few data to establish corroborations with CyTOF analyses (Data Supplement; Figures S26 and S27). Given the clinical information gained by pathologic assessment of post-treatment tumor biopsies, these should be considered in future trials to better understand the effect of our therapies.

In conclusion, our data reflect safety of the regimen and encouraging roles of H3.3K27M-specific $CD8^+$ T-cell responses in these patients, warranting further studies targeting the H3.3K27M epitope, such as a vaccine regimen with anti-PD1 therapy (based on expression of PD1 on H3.3K27M-reactive $CD8^+$ T-cells) and adoptive transfer of T-cells transduced with H3.3K27M-reactive T-cell receptor (4).

Methods

Study Design

PNOC007 (NCT 02960230) is a pilot trial assessing the safety, immunoreactivity, and efficacy of subcutaneous administration of the H3.3K27M synthetic peptide combined with helper TT peptide (Tet_{A830}, PolyPeptide, Inc.) (41, 42) emulsified in Montanide-ISA 51 VG (Seppic, Inc.) and in combination with poly-ICLC (Hiltonol ®, Oncovir, Inc.) in patients 3-21 years of age with newly diagnosed DIPG (Stratum A) or non-pontine DMGs, including spinal cord DMGs (Stratum B). Key inclusion criteria were the confirmation of HLA-A*02:01$^+$ status and the H3.3K27M mutation by CLIA-approved sequencing of tumor tissue as well as adequate organ function. Exclusion criteria included known immune system disorders and treatment with other investigational or anti-cancer agents with the exception of temozolomide (maximum 90 mg/m^2/dose) during focal radiation therapy (RT). Patients must have been either off systemic steroids or have been on a stable dose of dexamethasone not exceeding 0.1 mg/kg/day (maximum 4 mg/day). All patients were enrolled upon completion of focal RT.

Participating PNOC sites received the H3.3K27M synthetic peptide vaccine combined with TT peptide through a central supply from the Immunologic Monitoring and Cellular Products Lab at the University of Pittsburgh. Pharmacists at each site were trained for the emulsification process and prepared each vaccine emulsion (300 µg/dose H3.3K27M synthetic peptide and 200 µg/dose TT peptide in Montanide). The vaccine was administered subcutaneously in either the arm or thigh beginning 2-8 weeks after completion of RT and given every three weeks for the first eight doses followed by every six weeks (Data Supplement; Figure S28) on an outpatient basis for a maximum

treatment period of 96 weeks. Vaccine was administered at the same location unless prevented by adverse skin reaction. Concurrently, the adjuvant poly-ICLC was administered (30 μg/kg) intramuscularly within 2 cm from the vaccine injection site (43, 44). Follow-up data were collected through February 2020.

Study Assessments

Patients were monitored by laboratory assessments and physical examination. Tumor evaluations were performed with magnetic resonance imaging (MRI) at baseline and every 12 weeks. Blood was collected to assess circulating tumor DNA (ctDNA) at baseline, and every 12 weeks (10). Peripheral blood mononuclear cells (PBMCs) were collected at baseline and at weeks 12, 18, 24, then every 12 weeks thereafter for mass cytometry (CyTOF)-based immuno-monitoring assessments.

Central Imaging Review

A central radiology review of all cases was conducted retrospectively using RANO (45) criteria. MRI with T1 (with and without contrast-enhancement), T2, and T2 FLAIR (fluid-attenuated inversion recovery) was used to measure tumor size. Anterior-posterior and transverse dimensions were measured on the Horos (Horos Version 3.0) software package. Progressive disease on MRI was defined as >25% increase in the sum of perpendicular diameters and/or development of new enhancing or non-enhancing lesions by a board certified neuroradiologist (JVM).

Study Endpoints

Primary endpoints were evaluation of safety for all patients and OS at 12 months for patients enrolled in Stratum A. Exploratory endpoints included CyTOF-based evaluation of H3.3K27M-reactive $CD8^+$ T-cell responses in PBMC samples, immunohistochemistry of available tumor tissue, and ctDNA analyses.

Safety

Adverse events (AEs), serious adverse events (SAEs), and RLTs were reported from vaccine initiation to 30 days after last study treatment. Grading was based on CTCAE version 4.0 (46). RLTs were defined as any grade 2 or greater autoimmune reaction; any grade 3 or greater hematologic or non-hematologic toxicity with the exception of lymphopenia; any life-threatening event; and any other unexpected grade 2 or greater neurological deficit, which was related to the vaccine therapy and did not respond to a trial of dexamethasone or bevacizumab. AEs, SAEs, and RLTs were reviewed weekly by the study chairs (SM, HO) and PNOC leadership (SM, MP) per PNOC standardized operating procedures for safety monitoring. The Data Monitoring and Safety Committee (DSMC) at the University of California, San Francisco (UCSF) monitored the trial.
An early stopping rule was implemented based on RLT incidences as follows: the first 3 patients in each stratum were observed at least for 12 weeks before the next set of patients are enrolled. If a RLT occurred in 1 of the first 3 patients, an additional 3 patients would be enrolled in that stratum and observed for at least 12 weeks. If fewer than 2 of the first 6 patients in each stratum experienced a RLT with at least 12 weeks of follow-up, the remaining patients would be enrolled. If a RLT occurred in ≥ 2 of the first 6 patients, accrual would be suspended. Therefore, with six patients enrolled, there

is an 88% probability of detecting 1 or more RLTs with an underlying rate of 30%. There is a 74% probability of detecting 1 or more RLTs with an underlying rate of 20%. In strata A, if all 19 patients are enrolled there is an 86% probability of detecting 1 or more RLTs with an underlying rate of 10% and a 62% probability with an underlying rate of 5%.

Mass Cytometry Data Processing

Data acquisition for H3.3K27M epitope-specific $CD8^+$ T-cell responses was conducted using Fluidigm Helios CyTOF system at the UCSF Parnassus Flow Cytometry Core. The sensitivity and specificity of the HLA-A*02:01-H3.3K27M-dextramer (Immudex, Inc.) were validated by positive staining of $CD8^+$ T-cells transduced with an H3.3K27M-specific T-cell receptor (4) and negligible staining in non-transduced $CD8^+$ T-cells, respectively. H3.3K27M-reactive $CD8^+$ T-cells were pooled from all patients and displayed via a t-Distributed Stochastic Neighboring Embedding (tSNE) plot in the cytofkit package (47).

Statistics for OS and Immune Responses

For Stratum A, with a null hypothesis that OS12 is 40%, accrual of 19 patients provided 80% power with a target overall type I error of 0.05 to detect a 30% difference in OS12 using a one-sided exact binomial test. A null OS12 rate of 40% was chosen based on prior studies (48-50) and review of outcomes of DIPG patients. Time-to-event analyses were calculated using the Kaplan-Meier method from date of diagnosis to date of

censoring or death. Patients who withdrew consent, were lost to follow-up, or were still alive at the study cutoff date were censored for OS-based survival analyses. The Log-Rank and Likelihood-Ratio tests were used for comparison between groups in Kaplan-Meier and Cox Proportional Hazards Ratio (HR) analyses respectively. The Cox Proportional HR multivariate analyses used OS as the primary survival parameter and were conducted using non-confounding variables ($p>0.10$) as determined by Fisher's Exact Test. A P value of less than 0.05 was considered statistically significant.

For Stratum B, we obtained pilot OS data in this specific subpopulation to support the design of the subsequent phase 2 trial (n=10).

An overall immunological response to the vaccine was defined as at least a 25% post-vaccination increase in the proportion of H3.3K27M-reactive $CD8^+$ T-cells out of total live PBMCs relative to baseline. An analogous approach was used for classifying the expansion of tSNE-stratified bulk and H3.3K27M-reactive $CD8^+$ subpopulations.

Patients were further classified by relative abundance of PBMC-derived myeloid-derived suppressor cell (MDSC) subsets at baseline. Myeloid cells from all patients were pooled and stratified on a tSNE plot, revealing 32 discrete clusters (Data Supplement, Figure S14), of which, early (E-MDSC) and monocytic (M-MDSC) subsets (51) were quantified. Patients were assigned $MDSC^{hi}$ and $MDSC^{lo}$ designations based on the abundance of these populations relative to median levels at baseline. This approach was extrapolated to incorporate total (sum of E-MDSC and M-MDSC) MDSC levels.

Data analyses and visualization were performed using the ggplot2 (52) and cytofkit (47) R packages.

Study Approval

Prior to trial activation, appropriate approvals were obtained from relevant regulatory agencies, including the Food and Drug Administration (FDA) for the Investigational New Drug (IND# 17070) as well as local institutional review boards (IRB). All subjects or their parents gave informed consent and age-appropriate assent according to institutional IRB guidelines.

Acknowledgements

The authors thank the following individuals and organizations: study participants and their families, all PNOC staff for their assistance, all PNOC PIs supporting the study, the Immunologic Monitoring and Cellular Products Lab (IMCPL) at the University of Pittsburgh for preparation and distribution of the vaccine (supported in part by award P30 CA047904), UCSF Parnassus Flow Cytometry Core for mass cytometry-related services (P30 DK063720) and use of the CyTOF2 “Charmander” (S10 1S10OD018040-01), USCF data safety monitoring committee, Dr. Lawrence Fong and Cancer Immunotherapy Lab (CIL) at UCSF for processing and banking of patient-derived peripheral blood samples, Maryam Shahin for their contributions to the optimization of the CyTOF analytical platform, Marie-Eve Koziol SEPPIC Inc. for training research nurses for preparation of Montanide emulsions, and Drs. Nicholas Bayless and Pier Federico Gherardini at the Parker Institute for Cancer Immunotherapy (PICI) for computational analyses of mass cytometry data.

References

1. Hoffman LM, Veldhuijzen van Zanten SEM, Colditz N, Baugh J, Chaney B, Hoffmann M, Lane A, Fuller C, Miles L, Hawkins C, et al. Clinical, Radiologic, Pathologic, and Molecular Characteristics of Long-Term Survivors of Diffuse Intrinsic Pontine Glioma (DIPG): A Collaborative Report From the International and European Society for Pediatric Oncology DIPG Registries. *Journal of clinical oncology : official journal of the American Society of Clinical Oncology.* 2018;36(19):1963-72.
2. Schwartzentruber J, Korshunov A, Liu XY, Jones DT, Pfaff E, Jacob K, Sturm D, Fontebasso AM, Quang DA, Tonjes M, et al. Driver mutations in histone H3.3 and chromatin remodelling genes in paediatric glioblastoma. *Nature.* 2012;482(7384):226-31.
3. Wu G, Broniscer A, McEachron TA, Lu C, Paugh BS, Becksfort J, Qu C, Ding L, Huether R, Parker M, et al. Somatic histone H3 alterations in pediatric diffuse intrinsic pontine gliomas and non-brainstem glioblastomas. *Nature genetics.* 2012;44(3):251-3.
4. Chheda ZS, Kohanbash G, Okada K, Jahan N, Sidney J, Pecoraro M, Yang X, Carrera DA, Downey KM, Shrivastav S, et al. Novel and shared neoantigen derived from histone 3 variant H3.3K27M mutation for glioma T cell therapy. *J Exp Med.* 2018;215(1):141-57.
5. Keskin DB, Anandappa AJ, Sun J, Tirosh I, Mathewson ND, Li S, Oliveira G, Giobbie-Hurder A, Felt K, Gjini E, et al. Neoantigen vaccine generates intratumoral T cell responses in phase Ib glioblastoma trial. *Nature.* 2019;565(7738):234-9.
6. Khuong-Quang DA, Buczkowicz P, Rakopoulos P, Liu XY, Fontebasso AM, Bouffet E, Bartels U, Albrecht S, Schwartzentruber J, Letourneau L, et al. K27M mutation in histone

H3.3 defines clinically and biologically distinct subgroups of pediatric diffuse intrinsic pontine gliomas. *Acta Neuropathol.* 2012;124(3):439-47.

7. Solomon DA, Wood MD, Tihan T, Bollen AW, Gupta N, Phillips JJ, and Perry A. Diffuse Midline Gliomas with Histone H3-K27M Mutation: A Series of 47 Cases Assessing the Spectrum of Morphologic Variation and Associated Genetic Alterations. *Brain Pathol.* 2016;26(5):569-80.

8. Bonner ER, Saoud K, Lee S, Panditharatna E, Kambhampati M, Mueller S, and Nazarian J. *J Vis Exp*. 2019.

9. Panditharatna E, Kilburn LB, Aboian MS, Kambhampati M, Gordish-Dressman H, Magge SN, Gupta N, Myseros JS, Hwang EI, Kline C, et al. Clinically Relevant and Minimally Invasive Tumor Surveillance of Pediatric Diffuse Midline Gliomas Using Patient-Derived Liquid Biopsy. *Clinical cancer research : an official journal of the American Association for Cancer Research.* 2018;24(23):5850-9.

10. Mueller S, Jain P, Liang WS, Kilburn L, Kline C, Gupta N, Panditharatna E, Magge SN, Zhang B, Zhu Y, et al. A pilot precision medicine trial for children with diffuse intrinsic pontine glioma-PNOC003: A report from the Pacific Pediatric Neuro-Oncology Consortium. *International journal of cancer.* 2019;145(7):1889-901.

11. Karremann M, Gielen GH, Hoffmann M, Wiese M, Colditz N, Warmuth-Metz M, Bison B, Claviez A, van Vuurden DG, von Bueren AO, et al. Diffuse high-grade gliomas with H3 K27M mutations carry a dismal prognosis independent of tumor location. *Neuro-oncology.* 2018;20(1):123-31.

12. Pollack IF, Jakacki RI, Butterfield LH, Hamilton RL, Panigrahy A, Potter DM, Connelly AK, Dibridge SA, Whiteside TL, and Okada H. Antigen-specific immune responses and clinical outcome after vaccination with glioma-associated antigen peptides and polyinosinic-polycytidylic acid stabilized by lysine and carboxymethylcellulose in children with newly diagnosed malignant brainstem and nonbrainstem gliomas. *J Clin Oncol.* 2014;32(19):2050-8.

13. Ornatsky O, Bandura D, Baranov V, Nitz M, Winnik MA, and Tanner S. Highly multiparametric analysis by mass cytometry. *Journal of immunological methods.* 2010;361(1-2):1-20.

14. Saeys Y, Van Gassen S, and Lambrecht BN. Computational flow cytometry: helping to make sense of high-dimensional immunology data. *Nature reviews Immunology.* 2016;16(7):449-62.

15. Batard P, Peterson DA, Devevre E, Guillaume P, Cerottini JC, Rimoldi D, Speiser DE, Winther L, and Romero P. Dextramers: new generation of fluorescent MHC class I/peptide multimers for visualization of antigen-specific CD8+ T cells. *Journal of immunological methods.* 2006;310(1-2):136-48.

16. Dolton G, Lissina A, Skowera A, Ladell K, Tungatt K, Jones E, Kronenberg-Versteeg D, Akpovwa H, Pentier JM, Holland CJ, et al. Comparison of peptide-major histocompatibility complex tetramers and dextramers for the identification of antigen-specific T cells. *Clinical and experimental immunology.* 2014;177(1):47-63.

17. Tario JD, Jr., Chen GL, Hahn TE, Pan D, Furlage RL, Zhang Y, Brix L, Halgreen C, Jacobsen K, McCarthy PL, et al. Dextramer reagents are effective tools for quantifying CMV

antigen-specific T cells from peripheral blood samples. *Cytometry B Clin Cytom.* 2015;88(1):6-20.

18. Mastelic-Gavillet B, Balint K, Boudousquie C, Gannon PO, and Kandalaft LE. Personalized Dendritic Cell Vaccines-Recent Breakthroughs and Encouraging Clinical Results. *Front Immunol.* 2019;10(766.

19. Shimasaki N, Jain A, and Campana D. NK cells for cancer immunotherapy. *Nature reviews Drug discovery.* 2020.

20. Sahin U, and Tureci O. Personalized vaccines for cancer immunotherapy. *Science.* 2018;359(6382):1355-60.

21. Durgeau A, Virk Y, Corgnac S, and Mami-Chouaib F. Recent Advances in Targeting CD8 T-Cell Immunity for More Effective Cancer Immunotherapy. *Front Immunol.* 2018;9(14.

22. Kamphorst AO, Pillai RN, Yang S, Nasti TH, Akondy RS, Wieland A, Sica GL, Yu K, Koenig L, Patel NT, et al. Proliferation of PD-1+ CD8 T cells in peripheral blood after PD-1-targeted therapy in lung cancer patients. *Proceedings of the National Academy of Sciences of the United States of America.* 2017;114(19):4993-8.

23. Ma J, Zheng B, Goswami S, Meng L, Zhang D, Cao C, Li T, Zhu F, Ma L, Zhang Z, et al. PD1(Hi) CD8(+) T cells correlate with exhausted signature and poor clinical outcome in hepatocellular carcinoma. *Journal for immunotherapy of cancer.* 2019;7(1):331.

24. Sallusto F, Lenig D, Forster R, Lipp M, and Lanzavecchia A. Two subsets of memory T lymphocytes with distinct homing potentials and effector functions. *Nature.* 1999;401(6754):708-12.

25. van Duikeren S, Fransen MF, Redeker A, Wieles B, Platenburg G, Krebber WJ, Ossendorp F, Melief CJ, and Arens R. Vaccine-induced effector-memory CD8+ T cell responses predict therapeutic efficacy against tumors. *Journal of immunology.* 2012;189(7):3397-403.

26. Lieber S, Reinartz S, Raifer H, Finkernagel F, Dreyer T, Bronger H, Jansen JM, Wagner U, Worzfeld T, Muller R, et al. Prognosis of ovarian cancer is associated with effector memory CD8(+) T cell accumulation in ascites, CXCL9 levels and activation-triggered signal transduction in T cells. *Oncoimmunology.* 2018;7(5):e1424672.

27. Wistuba-Hamprecht K, Martens A, Heubach F, Romano E, Geukes Foppen M, Yuan J, Postow M, Wong P, Mallardo D, Schilling B, et al. Peripheral CD8 effector-memory type 1 T-cells correlate with outcome in ipilimumab-treated stage IV melanoma patients. *European journal of cancer.* 2017;73(61-70.

28. Kwok D, and Okada H. T-Cell based therapies for overcoming neuroanatomical and immunosuppressive challenges within the glioma microenvironment. *J Neurooncol.* 2020;147(2):281-95.

29. Nejo T, Yamamichi A, Almeida ND, Goretsky YE, and Okada H. Tumor antigens in glioma. *Semin Immunol.* 2020;47(101385.

30. Alban TJ, Alvarado AG, Sorensen MD, Bayik D, Volovetz J, Serbinowski E, Mulkearns-Hubert EE, Sinyuk M, Hale JS, Onzi GR, et al. Global immune fingerprinting in glioblastoma patient peripheral blood reveals immune-suppression signatures associated with prognosis. *JCI Insight.* 2018;3(21).

31. Weiss T, Vitacolonna M, and Zoller M. The efficacy of an IL-1alpha vaccine depends on IL-1RI availability and concomitant myeloid-derived suppressor cell reduction. *Journal of immunotherapy.* 2009;32(6):552-64.

32. Lee JM, Seo JH, Kim YJ, Kim YS, Ko HJ, and Kang CY. The restoration of myeloid-derived suppressor cells as functional antigen-presenting cells by NKT cell help and all-trans-retinoic acid treatment. *International journal of cancer.* 2012;131(3):741-51.

33. Song X, Guo W, Cui J, Qian X, Yi L, Chang M, Cai Q, and Zhao Q. A tritherapy combination of a fusion protein vaccine with immune-modulating doses of sequential chemotherapies in an optimized regimen completely eradicates large tumors in mice. *International journal of cancer.* 2011;128(5):1129-38.

34. Kotsakis A, Harasymczuk M, Schilling B, Georgoulias V, Argiris A, and Whiteside TL. Myeloid-derived suppressor cell measurements in fresh and cryopreserved blood samples. *Journal of immunological methods.* 2012;381(1-2):14-22.

35. Albeituni SH, Ding C, and Yan J. Hampering immune suppressors: therapeutic targeting of myeloid-derived suppressor cells in cancer. *Cancer journal.* 2013;19(6):490-501.

36. Lobon-Iglesias MJ, Giraud G, Castel D, Philippe C, Debily MA, Briandet C, Fouyssac F, de Carli E, Dufour C, Valteau-Couanet D, et al. Diffuse intrinsic pontine gliomas (DIPG) at recurrence: is there a window to test new therapies in some patients? *Journal of neuro-oncology.* 2018;137(1):111-8.

37. Yang F, Li Y, Zhang Q, Tan L, Peng L, and Zhao Y. The Effect of Immunosuppressive Drugs on MDSCs in Transplantation. *Journal of immunology research.* 2018;2018(5414808.

38. Zhao Y, Shen XF, Cao K, Ding J, Kang X, Guan WX, Ding YT, Liu BR, and Du JF. Dexamethasone-Induced Myeloid-Derived Suppressor Cells Prolong Allo Cardiac Graft Survival through iNOS- and Glucocorticoid Receptor-Dependent Mechanism. *Front Immunol.* 2018;9(282.

39. Jaimes C, Vajapeyam S, Brown D, Kao PC, Ma C, Greenspan L, Gupta N, Goumnerova L, Bandopahayay P, Dubois F, et al. MR Imaging Correlates for Molecular and Mutational Analyses in Children with Diffuse Intrinsic Pontine Glioma. *AJNR Am J Neuroradiol.* 2020;41(5):874-81.

40. Gupta N, Goumnerova LC, Manley P, Chi SN, Neuberg D, Puligandla M, Fangusaro J, Goldman S, Tomita T, Alden T, et al. Prospective feasibility and safety assessment of surgical biopsy for patients with newly diagnosed diffuse intrinsic pontine glioma. *Neuro-oncology.* 2018;20(11):1547-55.

41. Slingluff CL, Jr., Yamshchikov G, Neese P, Galavotti H, Eastham S, Engelhard VH, Kittlesen D, Deacon D, Hibbitts S, Grosh WW, et al. Phase I trial of a melanoma vaccine with gp100(280-288) peptide and tetanus helper peptide in adjuvant: immunologic and clinical outcomes. *Clin Cancer Res.* 2001;7(10):3012-24.

42. Okada H, Butterfield LH, Hamilton RL, Hoji A, Sakaki M, Ahn BJ, Kohanbash G, Drappatz J, Engh J, Amankulor N, et al. Induction of robust type-I CD8+ T-cell responses in WHO grade 2 low-grade glioma patients receiving peptide-based vaccines in combination with poly-ICLC. *Clin Cancer Res.* 2015;21(2):286-94.

43. Zhu X, Fallert-Junecko BA, Fujita M, Ueda R, Kohanbash G, Kastenhuber ER, McDonald HA, Liu Y, Kalinski P, Reinhart TA, et al. Poly-ICLC promotes the infiltration of effector T

cells into intracranial gliomas via induction of CXCL10 in IFN-alpha and IFN-gamma dependent manners. *Cancer Immunol Immunother.* 2010;59(9):1401-9.

44. Zhu X, Nishimura F, Sasaki K, Fujita M, Dusak JE, Eguchi J, Fellows-Mayle W, Storkus WJ, Walker PR, Salazar AM, et al. Toll like receptor-3 ligand poly-ICLC promotes the efficacy of peripheral vaccinations with tumor antigen-derived peptide epitopes in murine CNS tumor models. *JTranslMed.* 2007;5(10.

45. Wen PY, Macdonald DR, Reardon DA, Cloughesy TF, Sorensen AG, Galanis E, Degroot J, Wick W, Gilbert MR, Lassman AB, et al. Updated response assessment criteria for high-grade gliomas: response assessment in neuro-oncology working group. *J Clin Oncol.* 2010;28(11):1963-72.

46. Chen AP, Setser A, Anadkat MJ, Cotliar J, Olsen EA, Garden BC, and Lacouture ME. Grading dermatologic adverse events of cancer treatments: the Common Terminology Criteria for Adverse Events Version 4.0. *J Am Acad Dermatol.* 2012;67(5):1025-39.

47. Chen H, Lau MC, Wong MT, Newell EW, Poidinger M, and Chen J. Cytofkit: A Bioconductor Package for an Integrated Mass Cytometry Data Analysis Pipeline. *PLoS Comput Biol.* 2016;12(9):e1005112.

48. Bailey S, Howman A, Wheatley K, Wherton D, Boota N, Pizer B, Fisher D, Kearns P, Picton S, Saran F, et al. Diffuse intrinsic pontine glioma treated with prolonged temozolomide and radiotherapy--results of a United Kingdom phase II trial (CNS 2007 04). *European journal of cancer.* 2013;49(18):3856-62.

49. Janssen JM, Zwaan CM, Schellens JHM, Beijnen JH, and Huitema ADR. Clinical trial simulations in paediatric oncology: A feasibility study from the Innovative Therapies for Children with Cancer Consortium. *European journal of cancer.* 2017;85(78-85.

50. Cohen KJ, Heideman RL, Zhou T, Holmes EJ, Lavey RS, Bouffet E, and Pollack IF. Temozolomide in the treatment of children with newly diagnosed diffuse intrinsic pontine gliomas: a report from the Children's Oncology Group. *Neuro Oncol.* 2011;13(4):410-6.

51. Gabrilovich DI. Myeloid-Derived Suppressor Cells. *Cancer Immunol Res.* 2017;5(1):3-8.

52. Wickham H, and Grolemund G. *R for data science : import, tidy, transform, visualize, and model data.*

Table 1: Patient Baseline Characteristics

Characteristics	Whole Cohort (n=29)	DIPG (Stratum A; n=19)	Other DMG (Stratum B; n=10)
Median age (range), years	11 (5-18)	11 (5-17)	12 (7-18)
Female, No. (%)	16 (55%)	10 (53%)	6 (60%)
Location			
Pons	21	19	2 (with cerebellar/spinal cord)
Thalamic	6	0	7
Spinal cord	2	0	1
Race			
White	18	11	7
African American	2	1	1
Other	8	7	1
Declined	1	0	1
Ethnicity			
Non-Hispanic	23	14	9

Hispanic	3	3	0
Not available/declined	3	2	1
Median # of days from biopsy to start of RT (range)*	16 (2-49)	17 (4-25)	22 (range 2-49)
Median # of days from end of RT to first vaccine (range)	40 (22-71)	39 (27-71)	39 (22-53)
Median number of vaccines (range)	6 (1-11)	7 (2-11)	5 (1-11)
Positive H3.3K27 detection in plasma (% of available samples)	68.3% (41/60)	69.0% (29/42)	66.7% (12/18)

PBMC Immune profiling median # samples per patient (range)	2 (0-5)**	2 (1-5)	2 (0-3)
Steroid use yes (percent)	13 (45)	9 (47)	4 (40)
Temozolomide use during XRT yes (percent)	4 (13.8)	3 (15.8)	1 (10)
Off Study Treatment Criteria			
Progression	27	18	9
Lost to f/u; withdrawal of consent	1	0	1
Toxicity	1	1	0

Abbreviations: DIPG: Diffuse intrinsic pontine glioma; DMG: Diffuse Midline Glioma; RT: Radiation therapy; F/u: follow up

*Excluding one patient who had biopsy after start of radiation therapy

**One patient sample (PNOC007-16) lost due to technical difficulties during data acquisition

Table 2: H3.3K27M/TT related adverse events*

	Stratum A (n=19)		**Stratum B (n=10)**	
Any adverse event	416		182	
	Stratum A		**Stratum B**	
	Any grade	≥Grade 3	Any grade	≥Grade 3
Injection Site Reaction	27	1	8	0
Gastrointestinal disorders (Nausea, Vomiting/Diarrhea)	12	0	3	0
Fatigue	6	0	6	0
Fever	5	0	0	0
Nervous System related				
Gait disturbance	4	1	1	0
Muscle weakness	4	0	0	0
Abducens paresis	3	0	0	0
Ataxia	2	0	0	0
Glossopharyngeal nerve paresis	4	0	0	0
Headache	9	0	2	0
Paresthesia	3	0	1	0
Anorexia/Weight loss	3	0	2	0
Blood disorders				
Neutropenia	3	1	1	0
Lymphopenia	12	0	16	1
Leukopenia	8	0	12	0
Anemia	1	0	0	0
Laboratory investigations				
Hypokalemia	2	0	2	0
ALT increase	5	0	0	0
AST increase	4	0	0	0

*Occurring in more than one subject

Figure 1

Mass cytometry-based phenotyping of H3.3K27M-reactive CD8+ T-cell subpopulations reveal associations between immunological responses and prolonged overall survival (OS) or progression-free survival (PFS). (**A** and **B**) Kaplan-Meier survival curves contrasting the (**A**) OS and (**B**) PFS of patients enrolled into stratum A (*red*) and stratum B (*blue*) using log-rank tests. (**C**) *Left,* PBMCs derived from a healthy donor show absence of H3.3K27M dextramer staining*. Right,* H3.3K27M dextramer exhibits sensitive detection of H3.3K27M-specific TCR transduced CD8+ T-cells. (**D**) Heat map visualizing the relative expression (Z-score) of subpopulation markers in patient-derived H3.3K27M-reactive CD8+ T-cells. (**E**) Heat map visualizing the patient-specific presence (*blue*) or absence (*red*) of an expansion of H3.3K27M-reactive CD8+ T-cells in a subpopulation-specific manner. (**F** and **G**) Kaplan-Meier survival curves contrasting the (**F**) OS and (**G**) PFS of patients exhibiting an immunological response (*blue*) in comparison to patients that did not (*red*) using log-rank tests. (**H** and **I**) Kaplan-Meier survival curves contrasting the (**H**) OS and (**I**) PFS (*lower panel*) of patients exhibiting an expansion of effector memory H3.3K27M-reactive CD8+ T-cells (*blue*) in comparison to patients that did not (*red*) using log-rank tests.

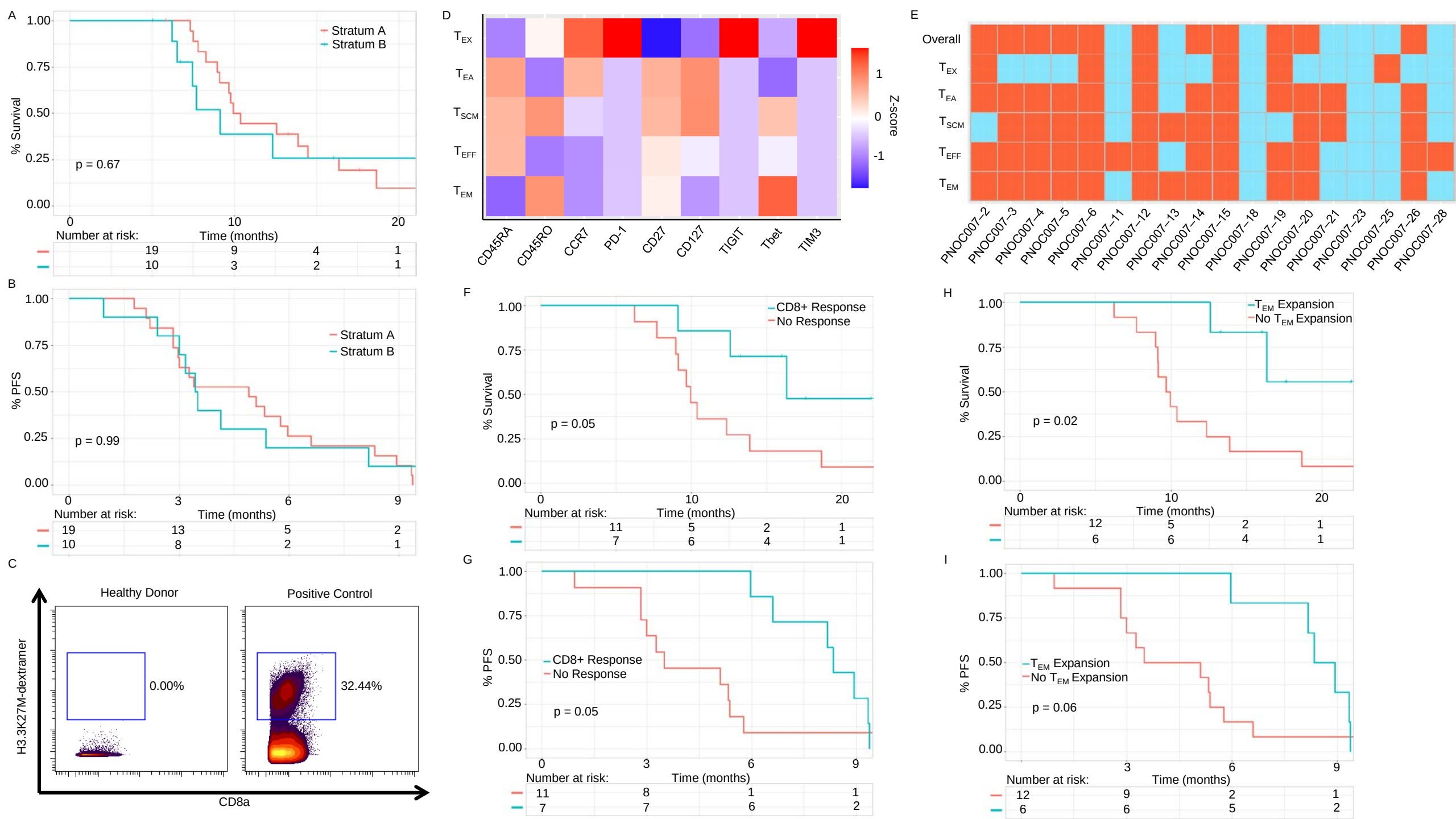
A
Stratum A
Stratum B
% Survival
p = 0.67
Number at risk:
Time (months)
19 9 4 1
10 3 2 1
B
Stratum A
Stratum B
% PFS
p = 0.99
Number at risk:
Time (months)
19 13 5 2
10 8 2 1
C
Healthy Donor
Positive Control
0.00%
32.44%
H3.3K27M-dextramer
CD8a
D
TEX
TEA
TSCM
TEFF
TEM
CD45RA
CD45RO
CCR7
PD-1
CD27
CD127
TIGIT
Tbet
TIM3
Z-score
E
Overall
PNOC007–2
PNOC007–3
PNOC007–4
PNOC007–5
PNOC007–6
PNOC007–11
PNOC007–12
PNOC007–13
PNOC007–14
PNOC007–15
PNOC007–18
PNOC007–19
PNOC007–20
PNOC007–21
PNOC007–23
PNOC007–25
PNOC007–26
PNOC007–28
F
CD8+ Response
No Response
% Survival
p = 0.05
Number at risk:
Time (months)
11 5 2 1
7 6 4 1
G
CD8+ Response
No Response
% PFS
p = 0.05
Number at risk:
Time (months)
11 8 1 1
7 7 6 2
H
TEM Expansion
No TEM Expansion
% Survival
p = 0.02
Number at risk:
Time (months)
12 5 2 1
6 6 4 1
I
TEM Expansion
No TEM Expansion
% PFS
p = 0.06
Number at risk:
Time (months)
12 9 2 1
6 6 5 2

Figure 2

Individual patient study course. Depicted within this swimmers plot is the patient-specific timing of vaccine administration, dexamethasone treatment, detection of H3.3K27M-reactive T-cell responses, tumor progression, and vital status (patient who withdrew consent were censored).

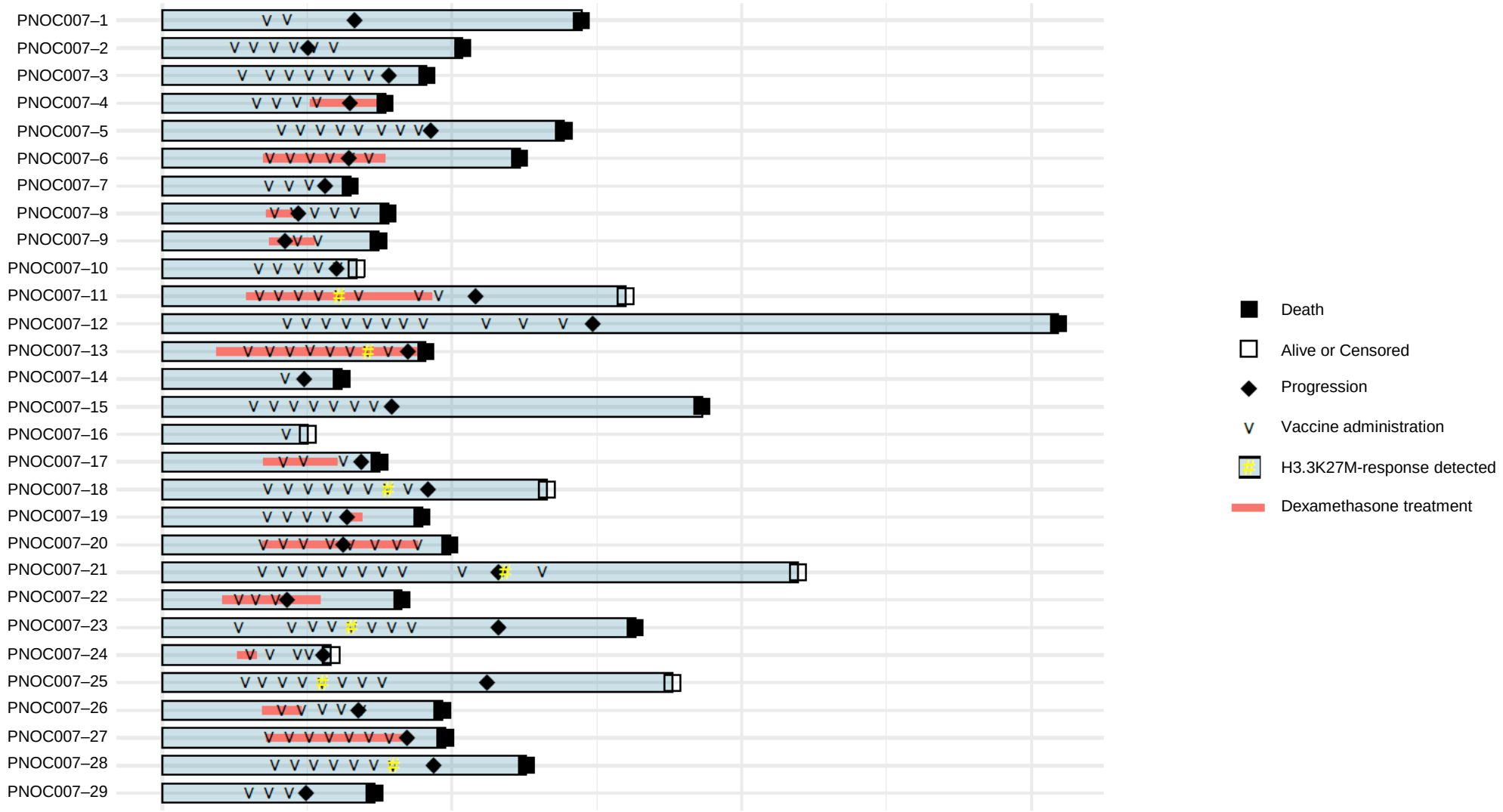
PNOC007–1
PNOC007–2
PNOC007–3
PNOC007–4
PNOC007–5
PNOC007–6
PNOC007–7
PNOC007–8
PNOC007–9
PNOC007–10
PNOC007–11
PNOC007–12
PNOC007–13
PNOC007–14
PNOC007–15
PNOC007–16
PNOC007–17
PNOC007–18
PNOC007–19
PNOC007–20
PNOC007–21
PNOC007–22
PNOC007–23
PNOC007–24
PNOC007–25
PNOC007–26
PNOC007–27
PNOC007–28
PNOC007–29
Death
Alive or Censored
Progression
Vaccine administration
H3.3K27M-response detected
Dexamethasone treatment

Figure 3

Mass cytometry-based analysis of circulatory myeloid-derived suppressor cells (MDSCs) reveal an association between baseline levels of MDSCs and shortened OS and PFS. (**A**) A representative gating strategy to identify myeloid cells from patient-derived PBMCs by mass cytometry. Cells stained double-positive with iridium intercalator were identified as intact cells (*left*). Cells with low cisplatin staining were identified as live cells (*second to left*). Cells staining negative for CD45 or positive for CD3 were excluded (*middle*). Cells staining positive for CD19 or positive for CD56 were excluded (*second to right*). Cells staining positive for either CD11b or CD11c were identified as myeloid cells (*right*). (**B**) Boxplot visualizing the range of abundance of circulatory total MDSCs among DIPG patients classified as $MDSC^{lo}$ and $MDSC^{hi}$. MDSC classifications were established based on a median threshold. (**C** and **D**) Kaplan-Meier survival curve contrasting the (**C**) OS and (**D)** PFS of DIPG patients with baseline circulatory MDSC levels above (*red*) and below (*blue*) the median threshold using log-rank tests.

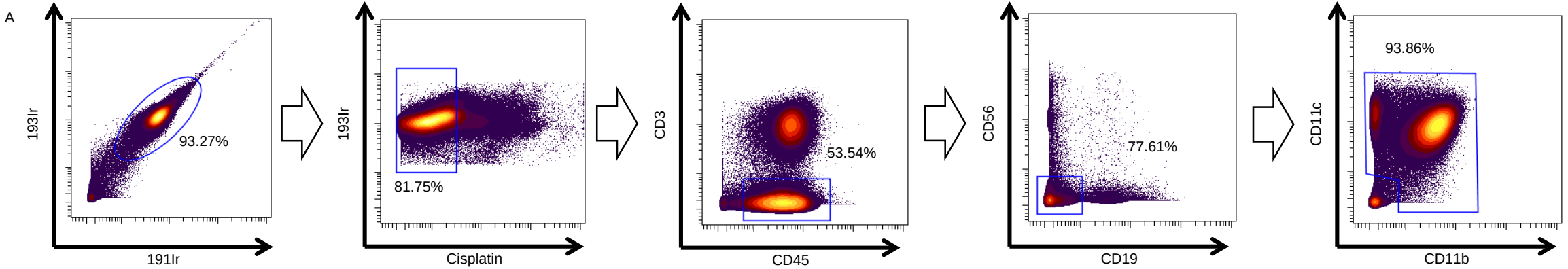
A
193Ir
191Ir
93.27%
193Ir
Cisplatin
81.75%
CD3
CD45
53.54%
CD56
CD19
77.61%
CD11c
CD11b
93.86%

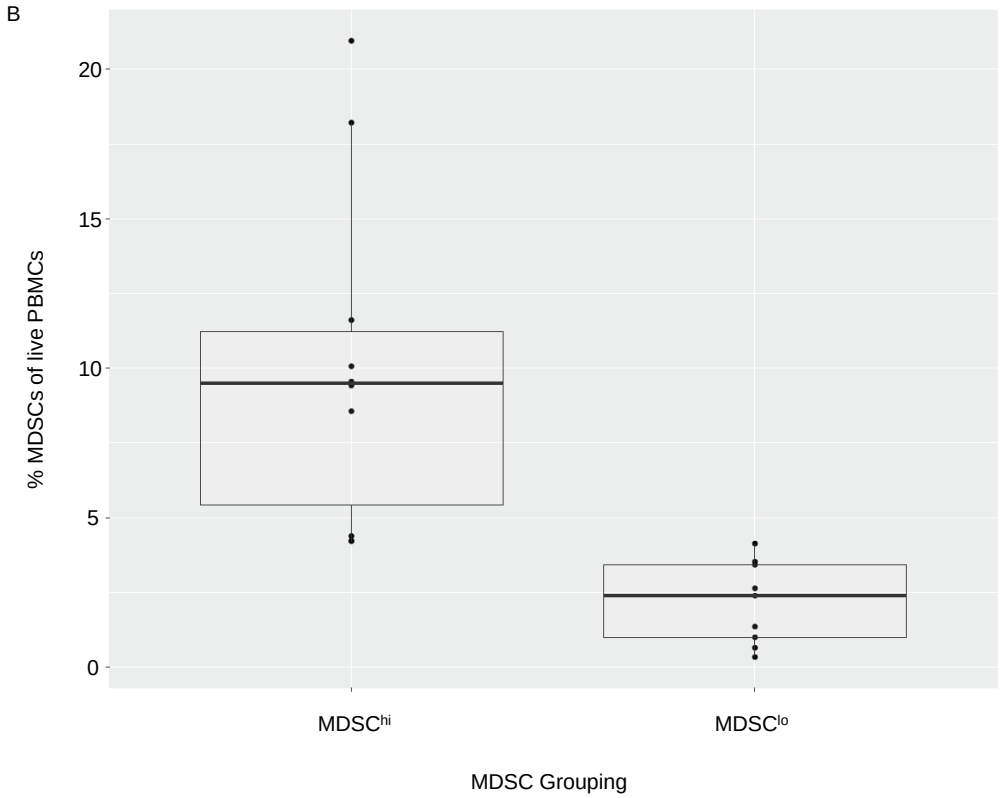
B
% MDSCs of live PBMCs
20
15
10
5
0
MDSC^hi
MDSC^lo
MDSC Grouping

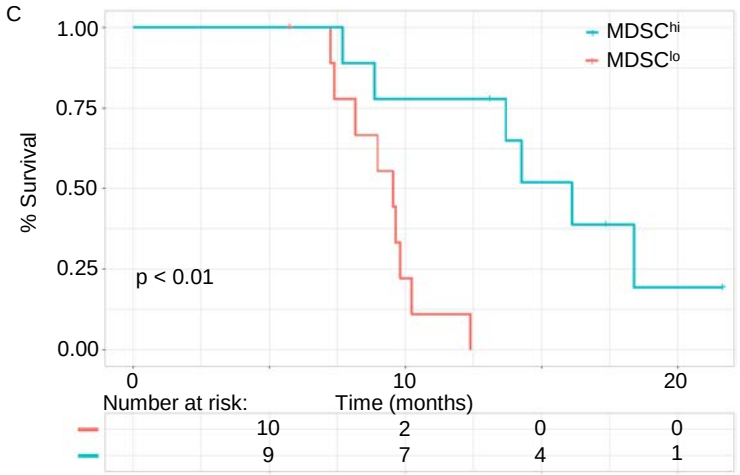
C
% Survival
1.00
0.75
0.50
0.25
0.00
p < 0.01
MDSC^hi
MDSC^lo
0
10
20
Number at risk:
Time (months)
10 2 0 0
9 7 4 1

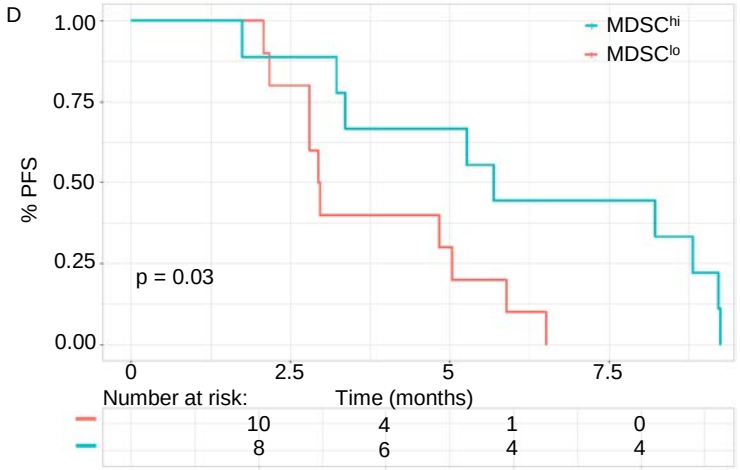
D
% PFS
1.00
0.75
0.50
0.25
0.00
p = 0.03
MDSC^hi
MDSC^lo
0
2.5
5
7.5
Number at risk:
Time (months)
10 4 1 0
8 6 4 4

Figure 4

Administration of dexamethasone is positively associated with increased baseline MDSC levels and inversely associated with H3.3K27M-reactive CD8+ T-cell responses and survival. (**A**) Boxplot visualizing the abundance of circulatory MDSCs at baseline among DIPG patients treated with dexamethasone (n=6) for at least three days prior to treatment relative to patients who did not receive dexamethasone (n=13). (**B**) Waterfall plot depicting the overall longitudinal percent change of H3.3K27M-reactive CD8+ T-cells at the final time point analyzed relative to baseline for each DIPG patient treated with dexamethasone. *Yellow,* pre-treatment, *red* patients receiving dexamethasone after commencement of vaccination, *blue* patients not receiving dexamethasone while on study. (**C** and **D**) Kaplan-Meier survival curves contrasting the (**C**) OS (*upper panel*) and (**D**) PFS (*lower panel*) of DIPG patients based on pre-treatment dexamethasone administration using log-rank tests.

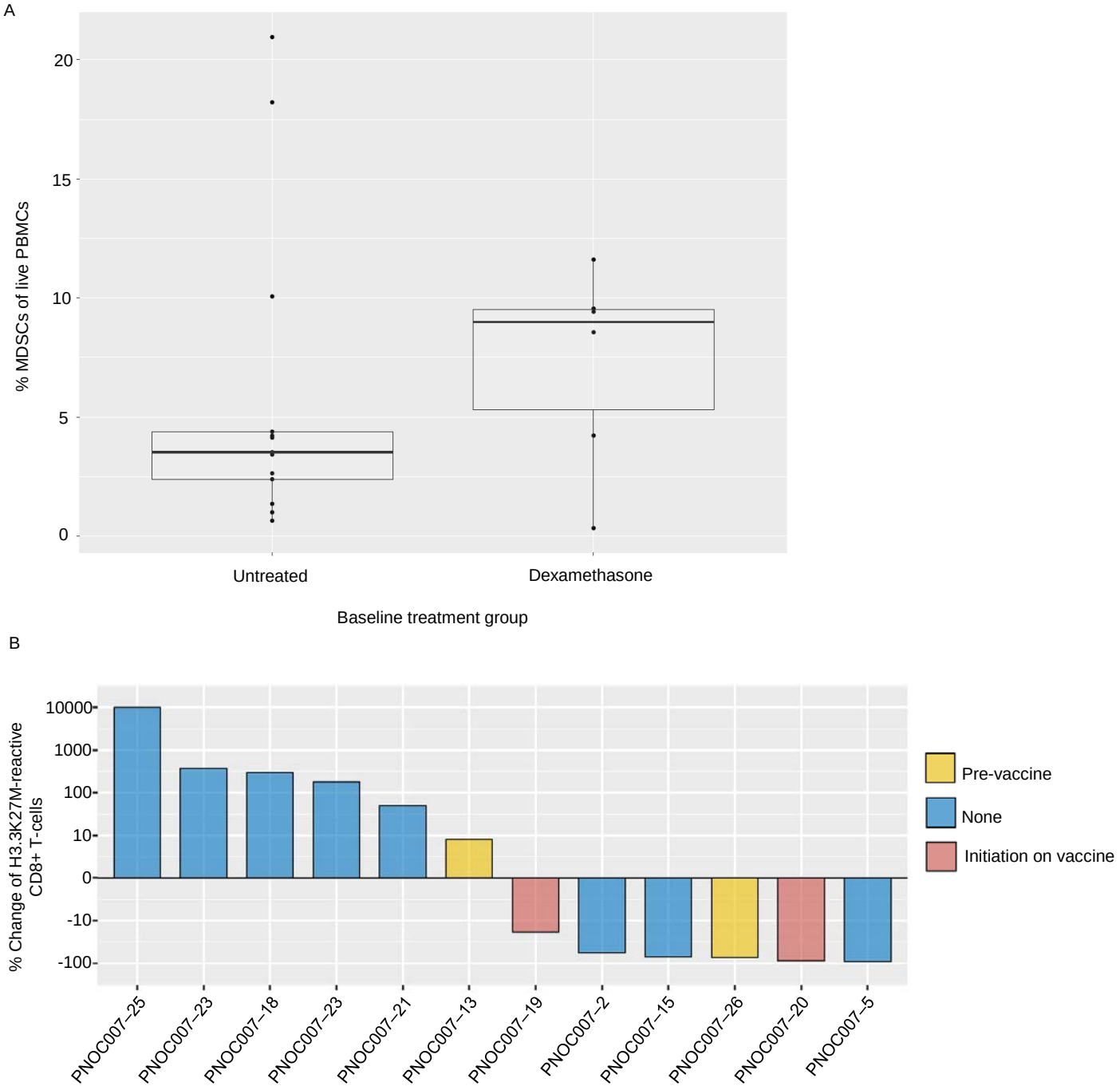
A
% MDSCs of live PBMCs
20
15
10
5
0
Untreated
Dexamethasone
Baseline treatment group
B
% Change of H3.3K27M-reactive CD8+ T-cells
10000
1000
100
10
0
-10
-100
PNOC007–25
PNOC007–23
PNOC007–18
PNOC007–23
PNOC007–21
PNOC007–13
PNOC007–19
PNOC007–2
PNOC007–15
PNOC007–26
PNOC007–20
PNOC007–5
Pre-vaccine
None
Initiation on vaccine
C
% Survival
1.00
0.75
0.50
0.25
0.00
p < 0.01
Dexamethasone
Untreated
0
10
20
Number at risk:
Time (months)
13 9 4 1
6 0 0 0
D
% PFS
1.00
0.75
0.50
0.25
0.00
p = 0.09
Dexamethasone
Untreated
0
2.5
5
7.5
Number at risk:
Time (months)
13 8 4 4
5 2 1 0

Figure 5

A patient who demonstrated a continued expansion of H3.3K27M-reactive CD8+ T-cells. (**A**) MR imaging of patient at baseline (*left*), week 12 (*second to left*), week 24 (*second to right*), and week 36 (*right*). The patient (PNOC007-25) underwent local progression at week 36. (**B**) Plot visualizing the longitudinal percent of H3.3K27M-reactive CD8+ T-cell subpopulations in live PBMCs. (**C**) Plot visualizing the longitudinal percent of circulatory MDSC subsets in live PBMCs.

A

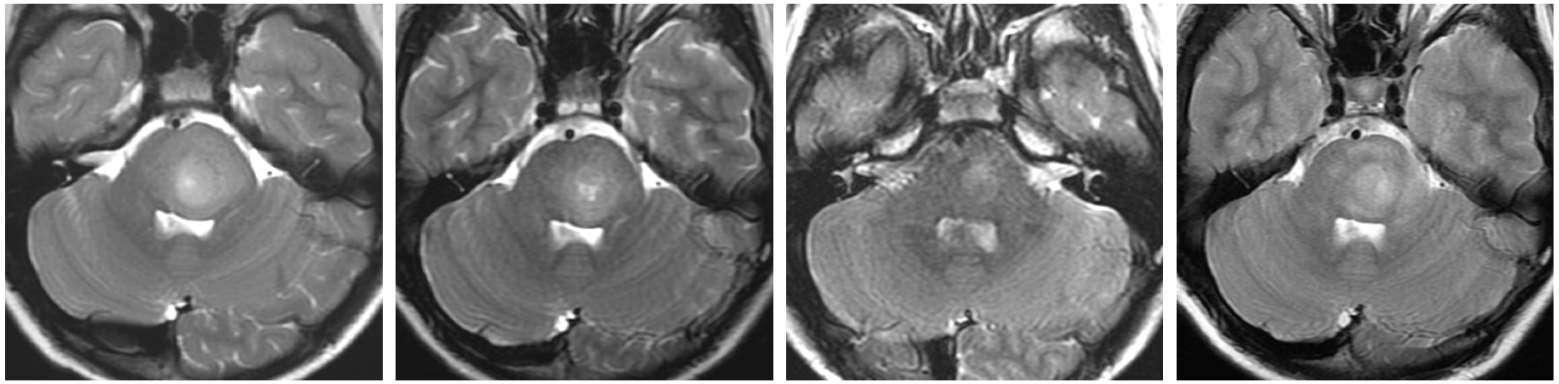

B

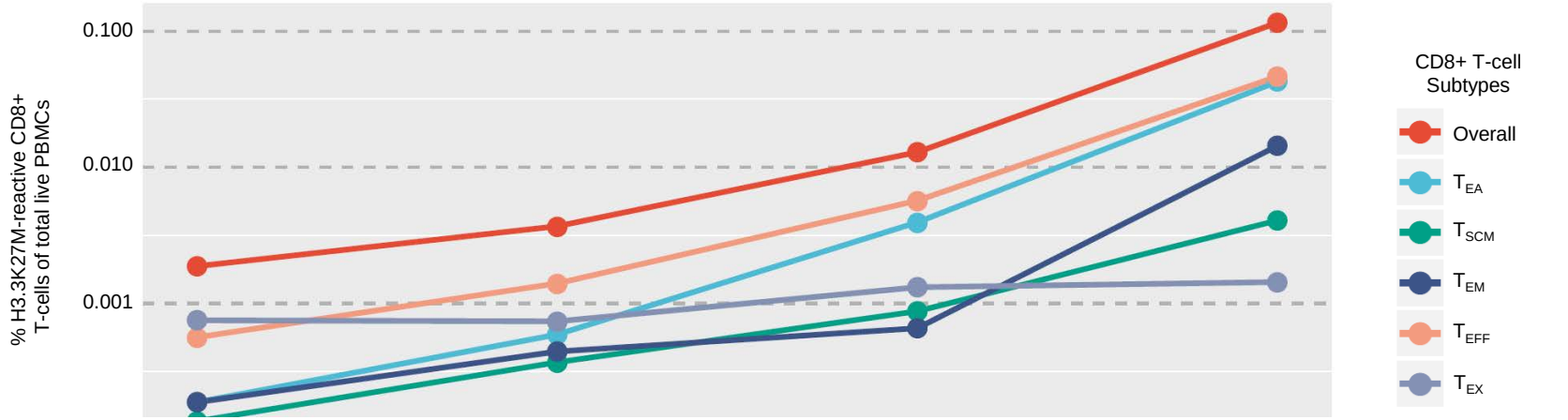
0.100
0.010
0.001
% H3.3K27M-reactive CD8+
T-cells of total live PBMCs
CD8+ T-cell
Subtypes
Overall
T_{EA}
T_{SCM}
T_{EM}
T_{EFF}
T_{EX}

C

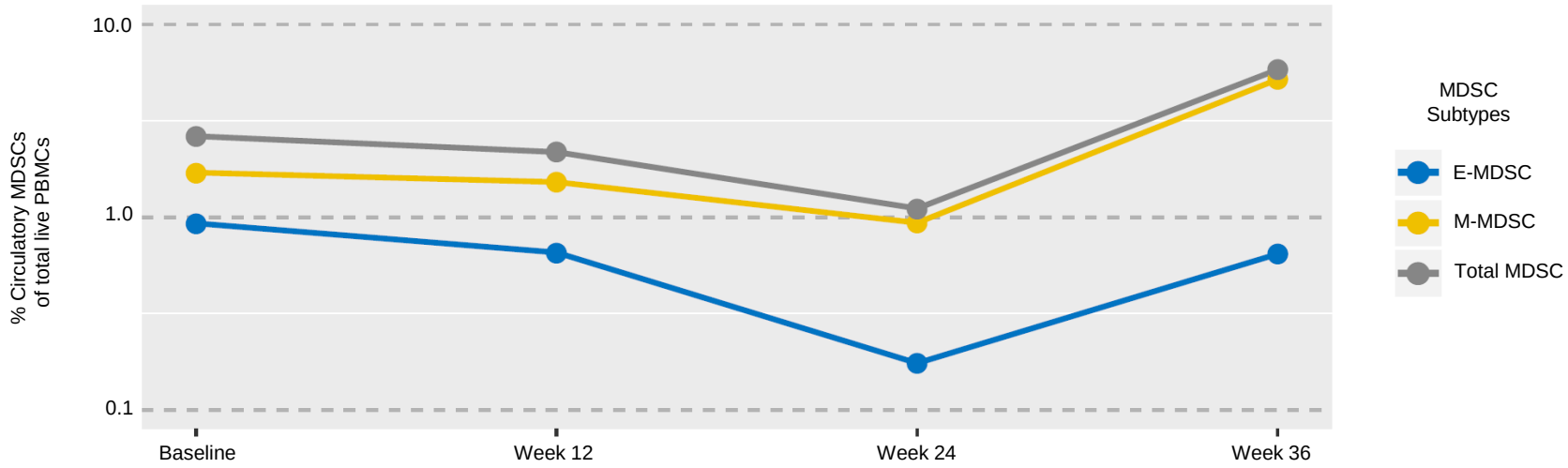
10.0
1.0
0.1
% Circulatory MDSCs
of total live PBMCs
MDSC
Subtypes
E-MDSC
M-MDSC
Total MDSC
Baseline
Week 12
Week 24
Week 36